A New Framework for Modelling and Analysing of Faulty Bearing Signals

A. HAD[1], K. SABRI[1]

[1]STIC laboratory, Department of Physics, Faculty of sciences,
University Chouaïb Doukkali, El Jadida, Morocco
had.a@ucd.ac.ma

Abstract

Over the past two decades, several models of a faulty bearing vibration signal have been proposed, and the majority of these models are assumed to be cyclostationary. To the best of our knowledge, all related works remain general whatever the nature of the bearing fault and with limited theoretical cyclic analysis. This study is a natural extension of previous related works which aims to provide a detailed and coherent theoretical framework allowing the correct description of inner-race and outer-race bearing fault signals. To do this, we propose a new mathematical model and prove analytically the property of wide-sense cyclostationarity. As a matter of fact, a good comprehension of bearing fault mechanism can allow the development of efficient algorithms for fault identification. Thus, this model and the corresponding theoretical development can be used as a platform for deconvolution, and blind source separation. In order to confirm the effectiveness of the theoretical cyclic analysis related to the proposed model, some simulations on synthetic and real faulty bearing signals are presented.

1 Introduction

It is well known that rolling element bearings are the most fragile components for rotating machines. Because of hostile working conditions, and other reasons, bearings usually are easily damaged. Those damages mainly result in vibrations and noise which can break the machine or at worst, bring down the whole system and then be the cause for much more economic losses. Actually, machine vibrations are an important source of information describing the machine state. Hence the need for tools to correctly extract and analyse this information. During the past fifty years, many monitoring and diagnostic techniques have been developed to detect bearing faults, from vibratory signals, before failure occurs. Thus, vibration analysis becomes the most used and suitable tool for bearing faults analysis.

When an outer-race or inner-race bearing fault occurs, a periodic impact is generated, which excites the resonance frequency of the mechanical system. Consequently, a spectral analysis of the recorded vibratory signal reveals that each element of the bearing is responsible for a unique frequency [1], identified as a bearing characteristic frequency (BCF), which are ball pass frequency of inner-race (BPFI), ball pass frequency of outer-race (BPFO), ball spin frequency (BSF), and fundamental cage frequency (FCF). However, the generated impulses are generally weak especially at early stage of bearing fault and are hidden in noise and other vibration sources. This makes the early fault identification more difficult.

Over the past two decades, several models of faulty bearing vibration signals have been proposed in order to validate the effectiveness of various signal processing methods and techniques. McFadden has proposed a model produced by a single point defect [2]. And soon afterwards, the model was extended to describe multiple point defects [3]. Braun's [1] has described the mechanism of the bearing signature generation, considering the effect of localised and distributed defect. To give the bearing signature signal a better shape and be more realistic, Braun introduced randomness on phase and amplitude in his model and multiplied each sinusoid with the Heaviside function. This allows the model to include the random slip of the element and the cage, for which it has been successfully used [4, 5, 6, 7].

In nature, many processes are generated by time-varying parameters, which results in fluctuation and randomness. Some processes encountered in different field, such as communication, telemetry, radar, sonar, as-

tronomy, and mechanics [8, 9, 10, 11], give rise to random data with time-periodic statistical characteristics, which are known as cyclostationary (CS) processes. As a matter of fact, cyclostationarity is useful to enhance the accuracy and reliabilities of information gleaned from noisy data sets. Thanks to Gardner and al. [12, 13] a lot of work and results were established, which has lead to greater achievement in the field of CS analysis .

A bearing fault vibration signal is, in fact, a series of quasi-periodic impact of random amplitude, modulated with the charge distribution in the case of inner-race defect. It is well known that the combination of periodic deterministic and random phenomena gives rise to a CS process. So, one can assume that bearing fault vibration signal is CS. McCormick [14] was the first to model bearing fault signal as CS process. Antoni and Randall [15] used the uncertainties of the magnitude and the phase of each impact, to describe cyclostationarity in faulty bearing signal. They have demonstrated that a bearing fault could be modelled as 2^{nd} order CS process. Although, the signals from a localised fault in a bearing are not truly CS, but could be described as $pseudo-cyclostationary$ [16, 17, 11]. After that, Antoni [18] proposed new methodologies for cyclostationarity-based diagnostics of rolling-element bearings. The statistics are obtained by ensemble averaging over an ensemble of realisations (detail are presented in [19, 20]).

To our knowledge, all related works remain general whatever the nature of the bearing default and with limited theoretical cyclic analysis. So, this work comes to complete previous related works and presents a detailed and coherent framework allowing the correct description of inner-race and outer-race bearing fault signals at the end of diagnostic. Actually, a good comprehension of bearing fault mechanism can allow the development of efficient algorithms for fault identification. Thus, this model and the corresponding theoretical development can be used as platform for deconvolution, blind source separation, ...

The remaining parts of this paper are outlined as follow. Section 2 concerns the theoretical framework, which sums up two parts. The first part presents the proposed model and the basic theoretical background concerning the mechanism of the bearing signature generation. In the second part, a CS analysis is established to validate the proposed model. To give our theoretical work much credibility some simulations on synthetic and real faulty bearing vibration signals are presented and studied in section 3. At last, section 4 gives conclusions.

2 Theoretical framework

2.1 Proposed mathematical model of faulty bearing signal

This section introduces an analytical model to generate inner-race and outer-race bearing fault signals. Having a consistent mathematical model that can simulate the vibration signals, with a certain degree of accuracy, is essential for various reasons. Firstly, modelling requires a better understanding of the phenomenon and an extensive background knowledge. Secondly, modelling helps in formalising and validating existing techniques and leads to the creation of new diagnostic tools.

According to McFadden [2], when the rolling element of bearing strikes a localised defect, an impact is generated. This impact is represented by the impulse function δ. To describe the severity of the defect the impulse function is randomly weighted by the coefficient a_i, which is supposed to follow a Gaussian law $\mathcal{N}(\mu_a, \sigma_a^2)$, where i denote the impact indices. The period between impacts is represented by λ.

For several impact

$$\sum_i a_i \delta(t - i\lambda) \tag{1}$$

The frequency of the impact $f_{imp} = 1/\lambda$ depends on the location of the defect. This frequency can be one of the bearing characteristic frequency, BPFI, BPFO, BSF, which are given by the following relationships:

$$BPFI = \frac{Z}{2f_{sh}}\left(1 + \frac{d}{D}cos\gamma\right) \tag{2}$$

$$BPFO = \frac{Z}{2f_{sh}}\left(1 - \frac{d}{D}cos\gamma\right) \tag{3}$$

$$BSF = \frac{Df_{sh}}{d}\left(1 - \frac{d^2}{D^2}cos^2\gamma\right) \tag{4}$$

Where f_{sh} is the shaft rotation frequency in Hz, d the diameter of rolling element,D the pitch diameter, Z is the number of rolling elements, and γ is the contact angle.

However, in the case of inner-race faults, the load distribution is taken into consideration. As shown in Fig. 1, the severity of the impact force changes periodically with every bearing revolution [16]. Consequently, the impulses generated by the defect will be modulated by the load distribution as follows:

$$\sum_i a_i \delta(t - i\lambda)(1 + k\cos(2\pi f_{sh} t)) = \sum_i a_i (1 + k\cos(2\pi f_{sh} i\lambda))\delta(t - i\lambda) \tag{5}$$

Where $f_{sh} = 1/T$ is the rotation frequency, and k represents the modulation rate. For a outer-race bearing defect the modulation rate k is null i.e $k = 0$.

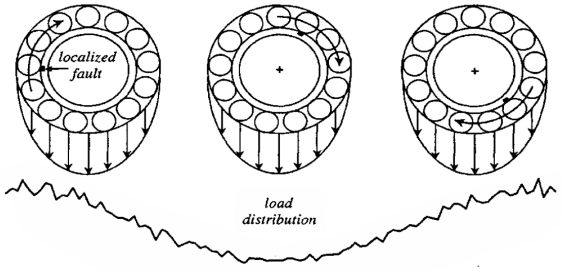

Figure 1 – The load disribution modulation for inner-race bearing fault.

Because of the distance between the accelerometer and the faulty bearing, the measured vibratory signal corresponds to the convolution between the modulated shocks and the impulse response of the mechanical structure. The impulse response $h(t)$ is generally assumed to be an exponential decaying sinusoid, oscillating with the resonance frequency f_{res}, and damped by the damping ratio ξ, with random phase fluctuation φ_i. Thus, the impulse response is given by the following relationship: $h(t) = e^{\frac{-\xi}{\sqrt{1+\xi^2}} 2\pi f_{res} t} \cos(2\pi f_{res} t - \varphi_i) u(t)$ where the Heaviside function is denoted by $u(t)$. Finally, the observed faulty bearing signal for a single impact is given by:

$$a_i(1 + k\cos(2\pi f_{sh} i\lambda))\, e^{\frac{-\xi}{\sqrt{1+\xi^2}} 2\pi f_{res}(t - i\lambda)} \cos(2\pi f_{res}(t - i\lambda)) - \varphi_i) u(t - i\lambda) \tag{6}$$

As the bearing rotates this process will be repeated for every impact as illustrated in Fig. 2. Thus, the final model is summarised as follows:

$$x_b(t) = \sum_i a_i(1 + k\cos(2\pi f_{sh} i\lambda))\, e^{\frac{-\xi}{\sqrt{1+\xi^2}} 2\pi f_{res}(t - i\lambda)} \cos(2\pi f_{res}(t - i\lambda)) - \varphi_i) u(t - i\lambda) \tag{7}$$

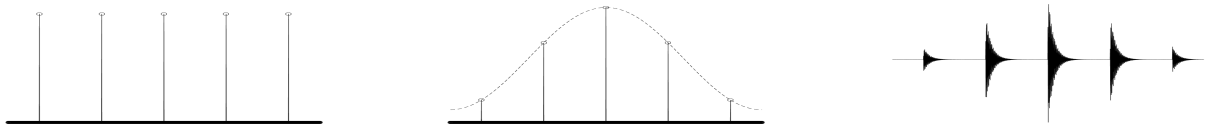

(a) (b) (c)

Figure 2 – Synthesis of the vibration signal produced by a localised bearing fault: (a) Series of impact forces with slight random fluctuations in their magnitudes. (b) Series of impact forces modulated by the charge distribution. (c) The measured noiseless signal.

The random fluctuation in $x_b(t)$ rises from the parameters a_i and φ_i. In fact, the amplitude a_i changes from one impact to another, and follows a Gaussian law $\mathcal{N}(\mu_a, \sigma_a^2)$. Whereas the random character of the phase φ_i, is due to the slip of rolling elements and other reasons. φ_i follows a uniform law inside the interval $[\varphi_0 - \Delta\varphi, \varphi_0 + \Delta\varphi]$ with $\Delta\varphi \in [0, \pi]$, and φ_0 is the balls initial phase.

The simulation of the proposed model of Eq. (7) is illustrated in Fig. 3, where the parameters values are listed in Tab. 1. Furthermore, the sampling frequency f_s is set to 10000 Hz.

As generally, the combination of periodic deterministic and random phenomena gives rise to a CS process. So, one can assume that bearing fault signals signal is CS. To confirm this hypothesis, we propose in the next section to prove analytically the property of wide-sense cyclostationarity of the model of Eq. (7) by computing cyclic statistics which are robust to stationary noise.

Parameter	μ_a (mv)	σ_a (mv)	k	f_{sh} (Hz)	λ (s)	f_{res} (Hz)	$\Delta\varphi$ (rad)	ξ	φ_0 (rad)
value	15	0.5	0.95	20	0.0105	1500 Hz	$\pi/10$	0.08	0.02

Table 1 – Model parameters values.

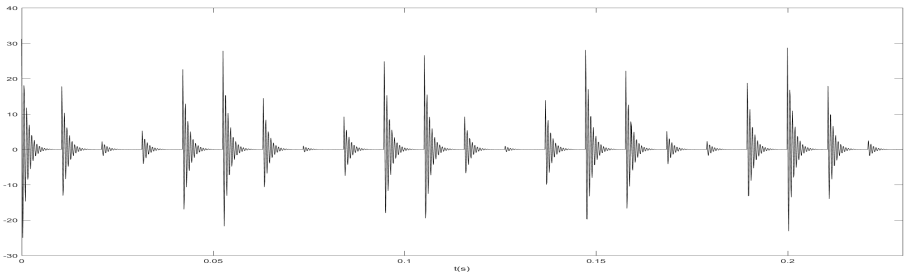

Figure 3 – Realistic synthetic bearing signal of inner-race fault.

2.2 Cyclic analysis

When a periodic phenomenon is affected by random fluctuation, it gives rise to CS process. Bearing fault vibration are known for presenting second order cyclostationarity [15]. Thus, a theoretical work has been established to prove the cyclostationarity of the proposed model in Eq. (7) .

Let x be a time dependent signal. x is said to be first-order CS if its first-order moment $m_x(t)$ is periodic with period T_0 [12] : $m_x(t) = \mathbb{E}(x(t)) = m_x(t+T_0)$. The First-order moment of the signal $x_b(t)$ given by the model of Eq. (7):

$$m_{x_b}(t) = \frac{\sin(\Delta\varphi)}{\Delta\varphi} \sum_i \mu_a (1 + k\cos(2\pi f_{sh} i\lambda))\, e^{\frac{-\xi}{\sqrt{1+\xi^2}} 2\pi f_{res}(t-i\lambda)} \cos(2\pi f_{res}(t-i\lambda) - \varphi_0) u(t-i\lambda) \tag{8}$$

From the equation above we can figure out that the first moment is not periodic with either λ or T. However, $m_{x_b}(t)$ is T_1-periodic where $T_1 = MT = N\lambda$ represent the lowest common multiple between T and λ. Hence, the periodicity of the first moment : $m_{x_b}(t+T_1) = m_{x_b}(t)$, affirm that $x_b(t)$ is 1^{st} order CS and T_1 represent the fundamental cyclic period. It should be noted that when $\Delta\varphi$ is close to 0, $m_{x_b}(t)$ converges to 0.

The process x is said to be wide sense CS if its mean $m_x(t)$ and time-varying autocorrelation function $R_x(t,\tau) = \mathbb{E}\{x(t-\tau/2)x^*(t+\tau/2)\}$, where the superscript * denotes complex conjugation, are periodic with the same period [12].

The time-varying autocorrelation function for the signal of the proposed model of Eq. (7), after removing the cyclic mean, is given by:

$$\begin{aligned} R_{x_b}(t,\tau) \quad &= \sum_i \frac{\sigma_a^2}{2}\left(1 + \frac{k^2}{2}\cos(2\pi f_{sh}\tau) + \frac{k}{2}\cos(\pi f_{sh}\tau)\cos(2\pi f_{sh} i\lambda)\right) + \frac{k^2}{2}\cos(4\pi f_{sh} i\lambda)\right)\, e^{\frac{-\xi}{\sqrt{1+\xi^2}} 4\pi f_{res}(t-i\lambda)} \\ &\quad [\cos(2\pi f_{res}\tau) + \frac{\sin(2\Delta\varphi)}{2\Delta\varphi}\cos(4\pi f_{res}(t-i\lambda) - 2\varphi_0)] u(t - i\lambda - \frac{|\tau|}{2}) \end{aligned} \tag{9}$$

As shown in Fig. 4 the time-varying autocorrelation function $R_x(t,\tau)$ is T_1-periodic too, which confirms the wide sense CS of x_b.

In the case of CS signals, in which the time-varying autocorrelation is T-periodic function, $R_x(t,\tau)$ can be represented by Fourier series $R_x(t,\tau) = \sum_\alpha R_x^\alpha(\tau) e^{j2\pi\alpha t}$, where R_x^α is the cyclic autocorrelation function (CAF).

The Fourier expansion of $R_x(t,\tau)$ can be expressed as :

$$\begin{cases} R_{x_b}^\alpha(\tau) = \sum_i \frac{\sigma_a^2}{2\lambda}[(1 + \frac{k^2}{2}\cos(2\pi f_{sh}\tau))G(\alpha,\tau) + \frac{k}{4}\cos(\pi f_{sh}\tau)\,(G(\alpha + f_{sh},\tau) + G(\alpha - f_{sh},\tau)) \\ \qquad\qquad + \frac{k^2}{4}\,(G(\alpha + 2f_{sh},\tau) + G(\alpha - 2f_{sh},\tau))]\delta(\alpha - i\lambda^{-1}) \\ G(\alpha,\tau) = e^{-(B4\pi f_{res} + j2\pi\alpha)|\tau|/2}\left(\frac{\cos(2\pi f_{res}\tau)}{B4\pi f_{res} + j2\pi\alpha} + \frac{\sin(2\Delta\varphi)}{4\Delta\varphi}\left(\frac{e^{j(4\pi f_{res}|\tau|/2 - 2\varphi_0)}}{B4\pi f_{res} - j4\pi(f_{res} - \alpha)} + \frac{e^{-j(4\pi f_{res}|\tau|/2 - 2\varphi_0)}}{B4\pi f_{res} + j4\pi(f_{res} + \alpha)}\right)\right) \end{cases} \tag{10}$$

where $B = \xi/\sqrt{1+\xi^2}$.

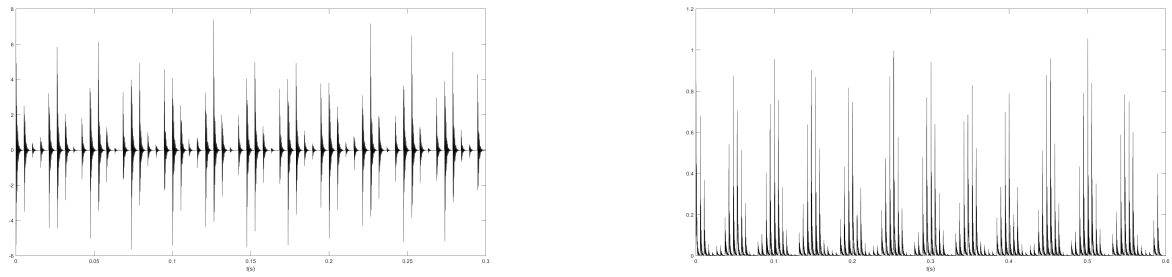

(a) (b)

Figure 4 – Numerical estimations of : (a) First order moment for inner-race bearing fault. (b) Time-varying autocorrelation for inner-race bearing fault for $\tau = 0$.

$R^{\alpha}_{x_b}(\tau)$ is α-discrete because $R_{x_b}(t,\tau)$ is T_1-periodic in time. Thus, the CAF is non zero only for the harmonics of $\alpha_1 = 1/T_1$. It should be noted that the amplitude variance σ_a, the phase $\Delta\varphi$, and the modulation rate k affect the cyclostationarity of the signal. Fig. 5-(a), illustrates the CAF of Eq. (10) for time lag $\tau \in [-0.003, 0.003]$. The CAF increases as the time-lag moves toward 0, the same process goes for α, where we find the maximum of $R^{\alpha}_{x_b}(\tau)$ in the center $(\alpha = 0, \tau = 0)$. Furthermore, high values of $R^{\alpha}_{x_b}(\tau)$ are detected for $\alpha = \pm 2 f_{res}$, where f_{res} represent the bearing resonance frequency.

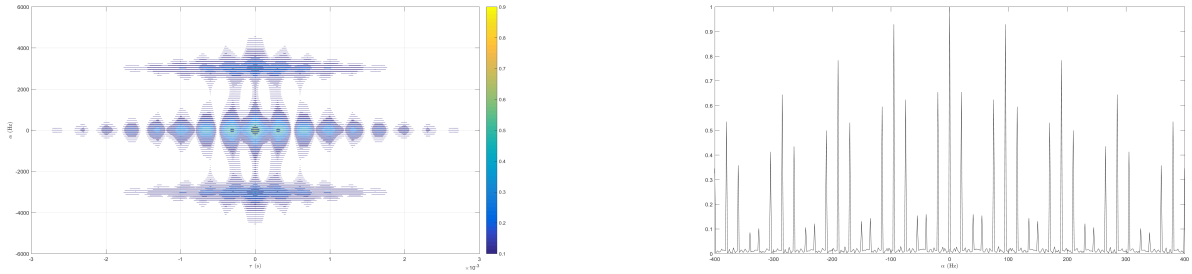

(a) (b)

Figure 5 – CAF for inner-race bearing fault : (a) Contour . (b) Upscaled CAF in α-plan for $\tau = 0$.

As a matching with Eq. (10), the CAF is non-zero for $f_{imp} = 1/\lambda$ multiples and its sidebands at $(if_{imp} \pm f_{sh})$ and $(if_{imp} \pm 2f_{sh})$ frequencies, which are α_1 multiples. Hence, the CAF is α-discretized by the fundamental cyclic frequency α_1 .The modulation effect is shown in Fig. 5-(b) where we find, f_{imp} distance between patterns, which represents the impact frequency, and five spikes in each pattern separated with f_{sh}. Those spikes around the central spikes are due to the term $(1 + kcos(2\pi f_{sh} i\lambda))$ in our model represented by Eq. (7). The fact that there is central spikes for the multiples of $\alpha = 95Hz$, where $f_{imp} = 95Hz$ represent BPFI of the bearing, make it clear that $\alpha = f_{imp}$ is the true cyclic period.

The cyclic spectral correlation (SCD) represents another important second-order cyclic statistic allowing the characterization in the (α, f)-plan. Gardner [12] defined $S^{\alpha}_{x_b}(f)$ as the Fourier transform of the CAF with respect to τ : $S^{\alpha}_{x_b}(f) = F(R^{\alpha}_{x_b}(\tau))$, where F denote the Fourier transform.

The Fourier transform of $R^{\alpha}_{x_b}(\tau)$ is equal to:

$$\begin{cases} S_{x_b}^{\alpha}(f) = \sum_i \frac{\sigma_a^2}{2\lambda}[G(\alpha,f) + \frac{k^2}{4}(G(\alpha,f-f_{sh}) + G(\alpha,f+f_{sh})) + \frac{k}{8}(G(\alpha+f_{sh},f-f_{sh}) + G(\alpha-f_{sh},f-f_{sh}) \\ \qquad +G(\alpha+f_{sh},f+f_{sh}) + G(\alpha-f_{sh},f+f_{sh})) + \frac{k^2}{4}(G(\alpha+2f_{sh},f) + G(\alpha-2f_{sh},f))]\delta(\alpha - i\lambda^{-1}) \\ \\ G(\alpha,f) = \frac{1}{B2\pi f_{res}+j\pi\alpha}\left(\frac{1}{B2\pi f_{res}-j2\pi(f-f_{res}-\alpha/2)} + \frac{1}{B2\pi f_{res}-j2\pi(f+f_{res}-\alpha/2)} + \frac{1}{B2\pi f_{res}+j2\pi(f-f_{res}+\alpha/2)} + \frac{1}{B2\pi f_{res}+j2\pi(f+f_{res}+\alpha/2)}\right) \\ \qquad + \frac{\sin(2\Delta\varphi)}{2\Delta\varphi}\left(\frac{e^{-j2\varphi_0}}{B2\pi f_{res}-j2\pi(f_{res}-\alpha/2)}\left(\frac{1}{B2\pi f_{res}-j2\pi(f+f_{res}-\alpha/2)} + \frac{1}{B2\pi f_{res}+j2\pi(f-f_{res}+\alpha/2)}\right)\right) \\ \qquad + \frac{\sin(2\Delta\varphi)}{2\Delta\varphi}\left(\frac{e^{j2\varphi_0}}{B2\pi f_{res}-j2\pi(f_{res}+\alpha/2)}\left(\frac{1}{B2\pi f_{res}-j2\pi(f+f_{res}+\alpha/2)} + \frac{1}{B2\pi f_{res}+j2\pi(f-f_{res}-\alpha/2)}\right)\right) \end{cases} \tag{11}$$

$S_{x_b}^{\alpha}(f)$ is α-discrete with non zero values for $\alpha = i\lambda^{-1}$ and its sidebands distanced by $\pm f_{sh}$ and $\pm 2f_{sh}$. It should be noted that $S_{x_b}^{\alpha}(f)$ is f-continous and present peaks in $\pm f_{res}$. Fig. 6-(a) reports the estimation of the SCD function . As illustrated in the figure, our model is proved as a second order CS process. The non-zero values of SCD are distributed in 4 regions, with maximums for $f = \pm f_{res}$. The two other regions are localised near $\alpha = \pm 2f_{res}$. Furthermore, SCD is reduced to the power spectral density when $\alpha = 0$.

As the CAF, the SCD is discretized in α-plan and is non-zero for the multiple of α_1. As shown in Fig. 6-(b), for $f = f_{res}$ we have the same distances between patterns $1/\lambda$, and $1/T$ between the five spikes in each pattern.

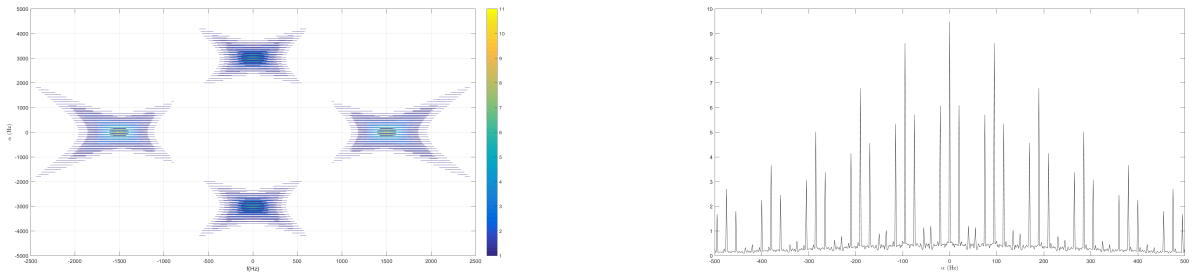

(a) (b)

Figure 6 – SCD estimation for inner-race bearing fault: (a) Contour . (b) Upscaled SCD in α-plan for $f = f_{res}$.

3 Simulation and experimental results

3.1 Synthetic bearing fault simulation

A simulation study is performed to illustrate the effectiveness of different bearing fault condition. For this purpose, two realistic synthetic signals are generated from Eq. (7) representing respectively inner-race fault bearing and outer-race fault bearing. The model parameters in Tab. 2, for both generated signal, were chosen to be similar with different modulation rate k, and different impact frequency f_{imp}. The outer-race bearing and the inner-race fault frequency are respectively equal to $f_{imp} = 82\ Hz$ and $f_{imp} = 120\ Hz$. The sampling frequency is set to $f_s = 48828 Hz$. Furthermore, some Gaussian noise is added to the signal such that the SNR is set to 10 dB.

Parameter	μ_a (mv)	σ_a (mv)	f_{sh} (Hz)	f_{res} (Hz)	$\Delta\varphi$ (rad)	ξ	φ_0 (rad)
value	7	1.5	25	1300	$\pi/20$	0.08	0.02

Table 2 – Model parameters values.

The simulated signals generated from the model of Eq. (7) are displayed in Fig. 7, where the modulation by the load distribution is visible.

The Fig. 8 gives the CAF estimation of both generated signals. The discretization in $\alpha - plan$ proves the cyclostationarity of the simulated inner-race and outer-race fault. As a matter of fact, The CAF estimation

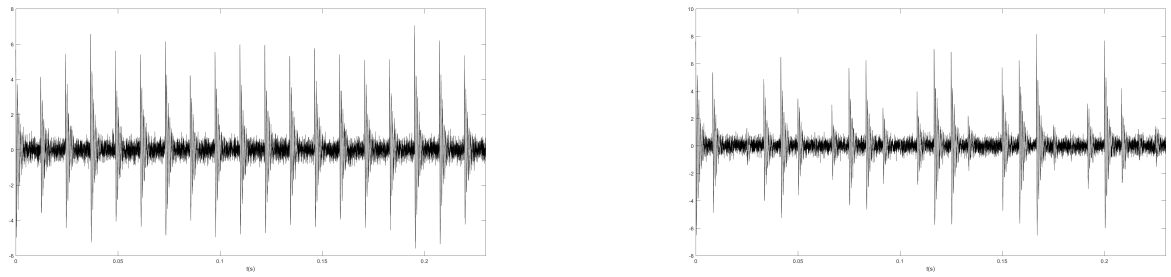

(a) (b)

Figure 7 – Synthetic bearing signals: (a) Outer-race fault ($k = 0$,$f_{imp} = 82Hz$). (b) Inner-race fault ($k = 0.9$,$f_{imp} = 120Hz$).

values is higher in the case of the generated inner-race fault bearing. This particularity can be explained by Eq. (10), where the terms $(1+k^2/2\cos(2\pi f_{sh}\tau))$, $(k/4\cos(\pi f_{sh}\tau))$, and $(k^2/4)$ increases as the modulation rate k increases with respect to τ. Furthermore, the CAF estimations are maximum for $\alpha = 0$ and present high peaks also for $\alpha = \pm 2f_{res}$, where f_{res} is the resonance frequency.

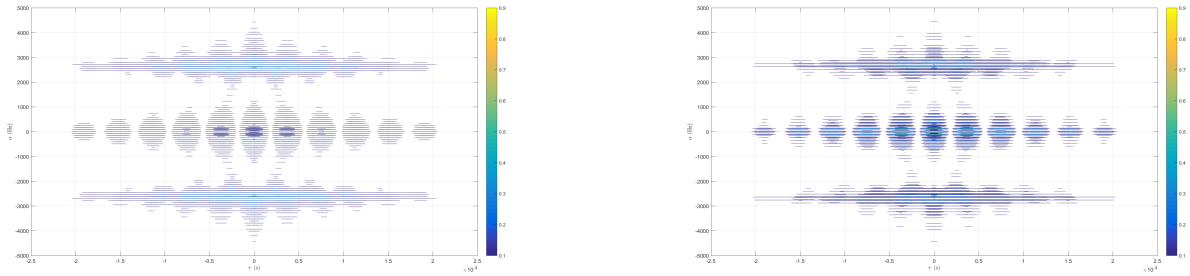

(a) (b)

Figure 8 – CAF estimation for synthetic bearing signals: (a) Outer-race fault (k=0). (b) Inner-race fault (k=0.65).

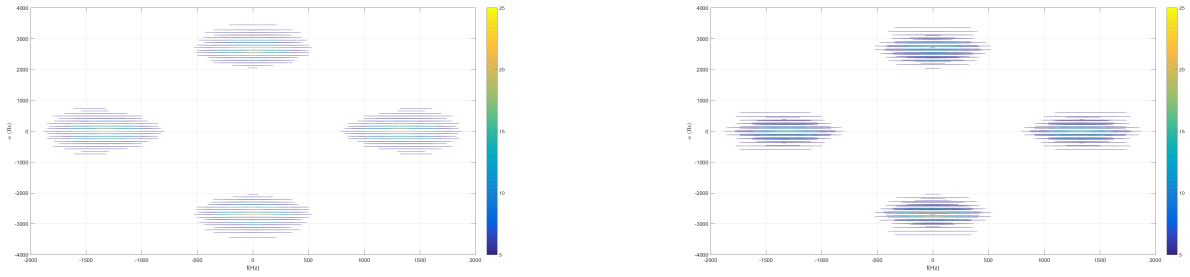

(a) (b)

Figure 9 – SCD estimation for synthetic bearing signals: (a) Outer-race fault (k=0). (b) Inner-race fault (k=0.65).

As illustrated by Fig. 9, the two SCD estimations are identical where the the high values are visible around $\alpha = \pm 2f_{res}$ along $f = 0Hz$ axis, and $f = \pm f_{res}$ in $\alpha = 0Hz$ axis. Due to the term $(k^2/4)$,and $(k/8)$ in Eq. (11) the modulation rate k increases the SCD estimation for inner-race bearing fault. However, in Fig. 10 the two upscaled SCD estimation in α-plan are different. For the outer-race bearing fault the modulation rate k is 0, which reduces the harmonics amplitude to 0. Therefore, The cyclic period will be the impact frequency f_{imp}.

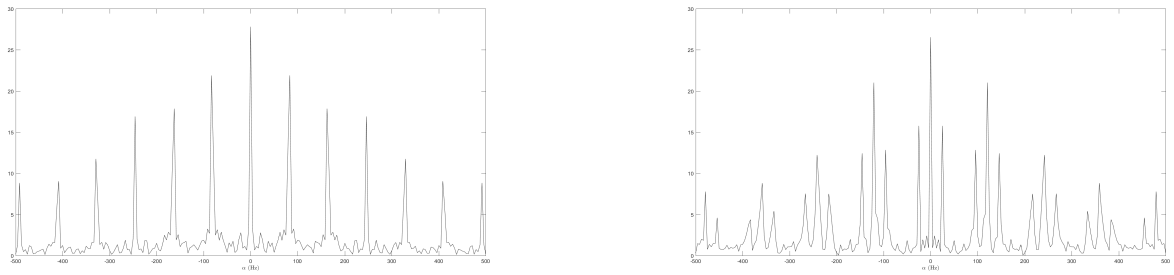

(a) (b)

Figure 10 – Upscaled SCD estimation for synthetic bearing signals: (a) Outer-race fault (k=0). (b) Inner-race fault (k=0.65).

3.2 Experimental results

This section aims at checking how the proposed model of Eq. (7) and the related cyclic statistics apply to real faulty bearing signals. In this experiment, a ball bearing has been overloaded on a test rig so that inner-race faults have developed. The settings of the experiment are listed in Tab. 3, and all experimental data of the real bearing signal has been assembled and prepared on behalf of MFPT, under the supervision of Dr. Eric Bechhoefer [21].

Parameter	value
Speed of shaft (Hz)	25
Bearing roller diameter (in)	0.235
Pitch circle diameter (in)	1.245
Number of rolling elements	8
Contact angle	0
Load (lbs)	0
Sampling frequency (kHz)	48.828
Record length (sample)	10000

Table 3 – Bearing characteristics and experiment settings.

The real inner-race bearing signal is displayed in Fig. 11, where the modulation by the load distribution is visible.

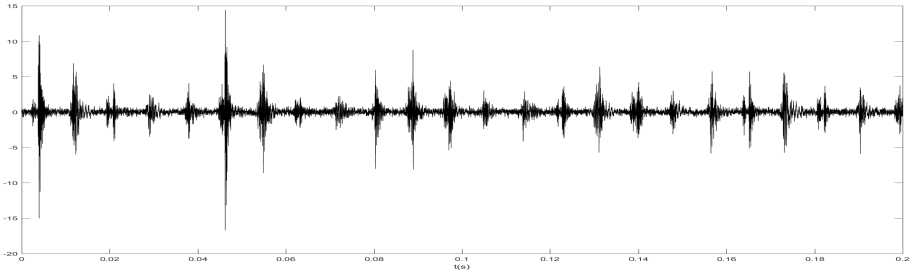

Figure 11 – Real inner-race bearing fault.

In similarity with the theoretical work, the CAF estimation of real bearing signal is maximum for $(\alpha = 0, \tau = 0)$, and decreases as we move away from the centre (Fig. 12-a). In fact, the CAF is non-zero for other values than $\alpha = 0$, which proves the cyclostationarity of the signal. Moreover, as described by Eq. (10) the CAF of the signal is α-discretized and presents high values around $\alpha = 0$, and $\alpha = \pm f_{res}$, where f_{res} is the resonance frequency.

In the case of inner-race bearing fault, the modulation ratio is different from zero which results, as described in Fig. 12-b, in four harmonics around each central spike distanced by the rotation frequency f_{sh}. Those central

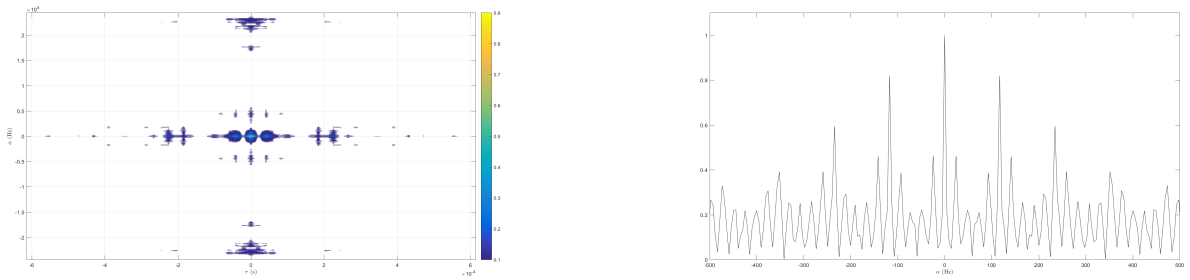

(a) (b)

Figure 12 – CAF estimation of real inner-race bearing fault: (a) CAF estimation for $\tau \in [-0.0006, 0.0006]$. (b) Upscaled CAF in α-plan for $\tau = 0$

spikes are the multiples of the impact frequency f_{imp}. The impact frequency is visibly identified and denotes the BPFI of the studied bearing, which is around $f_{imp} = 117Hz$.

It should be noted that the background noise is not stationary due to other machine vibration interference. As a result, the noise is not reduced by the cyclic statistical tools, which are robust to stationary noise. However, the results of this section are interesting and present similarities with our model, which proves the effectiveness of the proposed model for both inner-race and outer-race bearing fault vibrations.

4 conclusion

This paper proposes a new model for both inner-race and outer-race bearing fault vibration. This model is showed to be wide-sense CS process. Actually, the cyclostationarity of the proposed model is sensitive to the amplitude variance σ_a, the phase $\Delta\varphi$, and the modulation rate k. Due to CS tools, especially the CAF and SCD, hidden information can be extracted, which leads to fault detection despite stationary random noise. In fact, both simulated and experimental studies tools verify that, for low noise ratio, the CS tools can effectively extract the fault features of bearing. As a result, the proposed model presents similar statistical proprieties with the real inner-race bearing fault vibration, which confirms its robustness and coherence. Therefore, the proposed model could be used not only to validate existing techniques but also to develop new diagnostic tools in the future.

A future work will address the problem of deconvolution of faulty bearing signals, exploiting the cyclostationarity and the sparsity, in order to extract the exact fault frequency and other useful parameters for diagnostic tools.

References

[1] S. G. Braun. The signature analysis of sonic bearing vibrations. *IEEE Transactions on Sonics and Ultrasonics*, 27(6):317–327, Nov 1980.

[2] P.D. McFadden and J.D. Smith. Model for the vibration produced by a single point defect in a rolling element bearing. *Journal of sound and vibration*, 96(1):69–82, 1984.

[3] P.D. McFadden and J.D. Smith. The vibration produced by multiple point defects in a rolling element bearing. *Journal of sound and vibration*, 98(2):263–273, 1985.

[4] G. Dong, J. Chen, and Y. Ming. Feature extraction based on cyclic adaptive filter for gearbox fault diagnosis. In *9th WCEAM Research Papers*, 175–187. Springer, 2015.

[5] M. Zhao, J. Lin, X. Xu, and X. Li. Multi-fault detection of rolling element bearings under harsh working condition using imf-based adaptive envelope order analysis. *Sensors*, 14(11):20320–20346, 2014.

[6] K. F. Al-Raheem and W. Abdulkareem. Rolling element bearing fault diagnostics using laplace wavelet kurtosis. *IJMSE, World Academic Publishing*, 1(1):17–25, 2011.

[7] D. Wang, W. Guo, and X. Wang. A joint sparse wavelet coefficient extraction and adaptive noise reduction method in recovery of weak bearing fault features from a multi-component signal mixture. *Applied Soft Computing*, 13(10):4097–4104, 2013.

[8] S. Kazemi, A. Ghorbani, and H. Amindavar. Cyclostationary modelling of amplitude and frequency modulated signals in heart and respiration monitoring doppler radar systems. *IET Radar, Sonar Navigation*, 9(2):116–124, 2015.

[9] M. Nassar, A. Dabak, I. H. Kim, T. Pande, and B. L Evans. Cyclostationary noise modeling in narrowband powerline communication for smart grid applications. In *2012 IEEE International Conference on Acoustics, Speech and Signal Processing (ICASSP)*, 3089–3092, 2012.

[10] K. Sabri, M. El Badaoui, F. Guillet, A. Belli, G. Millet, and J. B. Morin. Cyclostationary modeling of ground reaction force signals. *Signal Processing*, 90(4):1146–1152, 2010.

[11] J. Antoni, F. Bonnardot, A. Raad, and M. El Badaoui. Cyclostationary modelling of rotating machine vibration signals. *Mechanical systems and signal processing*, 18(6):1285–1314, 2004.

[12] W. A. Gardner. Cyclostationarity in communications and signal processing. Technical report, DTIC Document, 1994.

[13] W. A. Gardner, A. Napolitano, and L. Paura. Cyclostationarity: Half a century of research. *Signal processing*, 86(4):639–697, 2006.

[14] A.C. McCormick and A.K. Nandi. Cyclostationarity in rotating machine vibrations. *Mechanical systems and signal processing*, 12(2):225–242, 1998.

[15] R.B. Randall, J. Antoni, and S. Chobsaard. The relationship between spectral correlation and envelope analysis in the diagnostics of bearing faults and other cyclostationary machine signals. *Mechanical Systems and Signal Processing*, 15(5):945 – 962, 2001.

[16] J. Antoni and R.B. Randall. A stochastic model for simulation and diagnostics of rolling element bearings with localized faults. *Journal of vibration and acoustics*, 125(3):282–289, 2003.

[17] J. Antoni and R.B. Randall. Differential diagnosis of gear and bearing faults. *Journal of Vibration and Acoustics*, 124(2):165–171, 2002.

[18] J. Antoni. Cyclic spectral analysis of rolling-element bearing signals: facts and fictions. *Journal of Sound and vibration*, 304(3):497–529, 2007.

[19] J. Antoni. Cyclic spectral analysis in practice. *Mechanical Systems and Signal Processing*, 21(2):597–630, 2007.

[20] J. Antoni. Cyclostationarity by examples. *Mechanical Systems and Signal Processing*, 23(4):987 – 1036, 2009.

[21] Eric Bechhoefer MFTP. Condition based maintenance fault database for testing of diagnostic and prognostics algorithms. `http://www.mfpt.org/FaultData/FaultData.htm`, 2013.